Available online at www.sciencedirect.com
SCIENCE DIRECT®
Inorganica Chimica Acta 350 (2003) 339–346
Inorganica Chimica Acta
www.elsevier.com/locate/ica

Cationic rhodium(I) complexes formed in the reactions of $HRh(CO)L_3$ ($L = PPh_3$, $P(OPh)_3$) complexes with silver(I) salts

Anna M. Trzeciak, Zofia Olejnik, Józef J. Ziółkowski *, Tadeusz Lis

Faculty of Chemistry, University of Wroclaw, 14 F. Joliot-Curie St., Wroclaw 50-383, Poland

Received 1 July 2002; accepted 25 September 2002

In honor of Professor Pierre Braunstein

Abstract

The reactions of $HRh(CO)L_3$ ($L = PPh_3$, $P(OPh)_3$) complexes with AgY ($Y = BF_4^-$, $CF_3SO_3^-$, PF_6^-) lead to $[Rh(CO)(PPh_3)_2(H_2O)]Y$ and $[Rh(CO)(P(OPh)_3)_3]Y$ compounds. The solvolysis of $[Rh(CO)(PPh_3)_2(H_2O)]PF_6$ in ethanol produced a crystalline *trans*-$[Rh(CO)(PPh_3)_2(OPOF_2)]$ complex containing distorted square-planar rhodium center. The different arrangement of $OPOF_2^-$ ligands found in two crystallographically independent molecules is connected with the presence of intra- and intermolecular C–H...O hydrogen bonds involving both oxygen atoms of each $OPOF_2^-$ anion. The reaction of $[Rh(CO)(P(OPh)_3)_3]Y$ ($Y = BF_4^-$, PF_6^-) in solution with CO leads to $[Rh(CO)_2(P(OPh)_3)_3]Y$ and with $P(OPh)_3$ to $[Rh(P(OPh)_3)_4]Y$ complexes. The $[Rh(P(OPh)_3)_4]PF_6$ complex was also obtained as a final reaction product of $HRh(P(OPh)_3)_4$ with $AgPF_6$.

Keywords: Hydridorhodium(I) complexes; Rhodium(II) complexes; Cationic Rh(I) complexes

1. Introduction

Hydridocarbonyl rhodium(I) complexes of $HRh(CO)L_3$ formula ($L = PPh_3$, $P(OPh)_3$) are well known as catalyst precursors or intermediates in hydroformylation, isomerization, and hydrogenation reactions of unsaturated substrates [1–3].

The electrochemical oxidation of $HRh(CO)(PPh_3)_3$ has been studied very carefully by different research groups [4–6]. It was found that one-electron oxidation leads to 17-electron monomeric cationic species $[HRh(CO)(PPh_3)_3]^+$ of square-pyramidal structure with a phosphorus atom in apical position [4]. The electron spin resonance (ESR) as well as UV–Vis spectra of $[HRh(CO)(PPh_3)_3]^+$ have been reported [4]. Further oxidation led to $[HRh(CO)(PPh_3)_3]^{2+}$, which undergoes deprotonation forming finally $[Rh(CO)(PPh_3)_3]^+$-type complexes [4,5], which have been identified only in solution by comparison with samples obtained by another route [7,8]. The products of electrochemical oxidation of $HRh(CO)(PPh_3)_3$ have never been isolated in solid.

In this paper, we present the studies of the reactions of $HRh(CO)L_3$ ($L = PPh_3$, $P(OPh)_3$) complexes with chemical oxidants, Ag(I) salts, performed with the aim to isolate the final reaction products. On the basis of literature data cited above, it was expected that in both reactions, of phosphino and phosphito hydridocarbonyls, cationic complexes of $[Rh(CO)L_3]^+$-type would be obtained and isolated. As far as we know, the preparation of $[Rh(CO)(P(OPh)_3LI)_3]^+$ complexes was not reported until now.

2. Results and discussion

2.1. Reaction of $HRh(CO)(PPh_3)_3$ complex with AgY ($Y = PF_6^-$, $CF_3SO_3^-$, BF_4^-)

Reactions of $HRh(CO)(PPh_3)_3$ complex with AgY salts ($Y = PF_6^-$, BF_4^-, $CF_3SO_3^-$) in CH_2Cl_2 solution were studied at room temperature at different [Ag]:[Rh] ratios (ranging from 0.5 to 2.5). In all experiments, the

* Corresponding author. Tel.: +48-71-375 7356; fax: +48-91-375 7356.
E-mail address: jjz@wchuwr.chem.uni.wroc.pl (J.J. Ziółkowski).

0020-1693/03/$ - see front matter © 2003 Elsevier Science B.V. All rights reserved.
doi:10.1016/S0020-1693(02)01551-7

formation of silver metal precipitate confirmed the occurrence of a redox process. The final products of the reactions of $HRh(CO)(PPh_3)_3$ with Ag(I) salts were complexes $[Rh(CO)(PPh_3)_2(H_2O)]Y$ formula ($Y = PF_6^-$, BF_4^-, $CF_3SO_3^-$) characterized by ^{31}P NMR and IR spectra (reaction (1)). The spectroscopic data were compared with those of $[Rh(CO)(PPh_3)_2(H_2O)]Y$ ($Y = CF_3SO_3^-$, BF_4^-) complexes obtained earlier by another route, in reactions of $RhCl(CO)(PPh_3)_2$ with respective AgY salts [9]. According to literature data [9], complexes with $Y = CF_3SO_3^-$ and BF_4^- ligands exist as aqua complexes of the $[Rh(CO)(PPh_3)_2(H_2O)]Y$-type; however, the existence of $[Rh(CO)(PPh_3)_2(SO_3CF_3)]$ has also been reported [10].

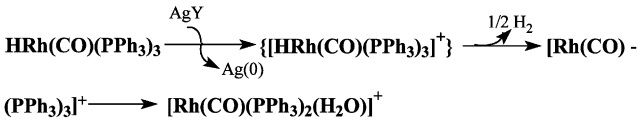

(1)

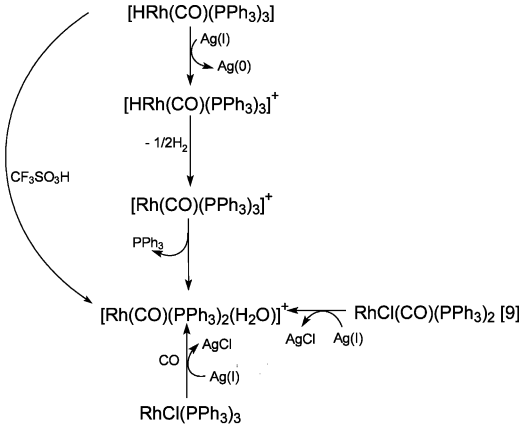

Scheme 1.

The water molecule in coordination sphere of rhodium origins from hygroscopic silver (I) salts used as oxidants.

By recrystallization of the crude product of the reaction of $HRh(CO)(PPh_3)_3$ with $AgPF_6$ from not carefully dried ethanol, $Rh(CO)(PPh_3)_2(OPOF_2)$ complex was obtained and its structure was determined by X-ray structural analysis (Fig. 1). This complex was obtained and characterized earlier; however, X-ray data were not published [9]. The solvolysis of the PF_6^- ligand and $OPOF_2^-$ anion formation were already reported for other systems [9,11–13].

It was surprising that in the reaction of $HRh(CO)(PPh_3)_3$ with AgY salts, we obtained $[Rh(CO)(PPh_3)_2(H_2O)]^+$ cationic species as final products instead of expected $[Rh(CO)(PPh_3)_3]^+$. Therefore, for comparison, the reaction of $RhCl(PPh_3)_3$ with $Ag(CF_3SO_3)$ was studied (see Scheme 1).

It was expected that this reaction performed in the presence of CO (1 atm) would produce

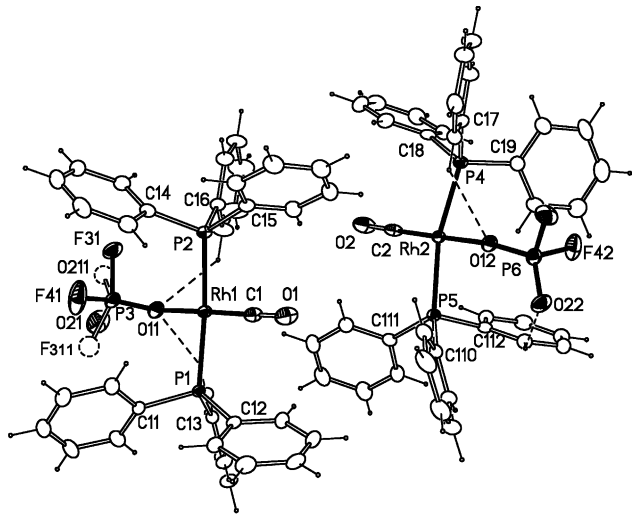

Fig. 1. The packing fragment showing two independent molecules of *trans*-$Rh(CO)(PPh_3)_2(OPOF_2)$ with 50% ellipsoids. The intramolecular C–H...O hydrogen bonds are marked by dashed lines. The dotted circles represent the minor component of the disordered $OPOF_2^-$ group.

$[Rh(CO)(PPh_3)_3](CF_3SO_3)$ complex. The isolated rhodium complex was, however, identified as $[Rh(CO)(PPh_3)_2(H_2O)](CF_3SO_3)$ by the characteristic doublet in ^{31}P NMR ($\delta = 29.8$ ppm, $J(Rh–P) = 124$ Hz) (reaction (2)):

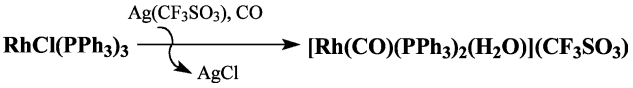

(2)

The same product was also obtained in the reaction of $HRh(CO)(PPh_3)_3$ with triflic acid (reaction (3)):

$$HRh(CO)(PPh_3)_3 + CF_3SO_3H \rightarrow [Rh(CO)(PPh_3)_2(H_2O)](CF_3SO_3) + H_2 \quad (3)$$

Reaction (1) of $HRh(CO)(PPh_3)_3$ with AgY salt was monitored using the IR spectra measurements and the representative results obtained at the concentration ratio [Ag]:[Rh] = 0.7 are shown in Fig. 2. Immediately (ca. 2 min) after the addition of solid $HRh(CO)(PPh_3)_3$ to the solution of silver salt in CH_2Cl_2, the ν(CO) band at 1920 cm^{-1} and the ν(Rh–H) band at 2006 cm^{-1}, originating from the starting complex, disappeared and a new ν(CO) band at 2000 cm^{-1} was observed. When instead of $HRh(CO)(PPh_3)_3$, its deuterated analogue, $DRh(CO)(PPh_3)_3$ (ν(CO) 1960 cm^{-1}), was used, the band at 2000 cm^{-1} was also observed at the beginning of the reaction. This new ν(CO) frequency, which intensity decreased in time, was assigned to the unstable Rh(II) cationic complex, $[HRh(CO)(PPh_3)_3]^+$ (reaction (1)). Decomposition of $[HRh(CO)(PPh_3)_3]^+$ led to $[Rh(CO)(PPh_3)_3]^+$ complex, evidenced by the appearance of a new ν(CO) band at 1970 cm^{-1} (Fig. 2). The

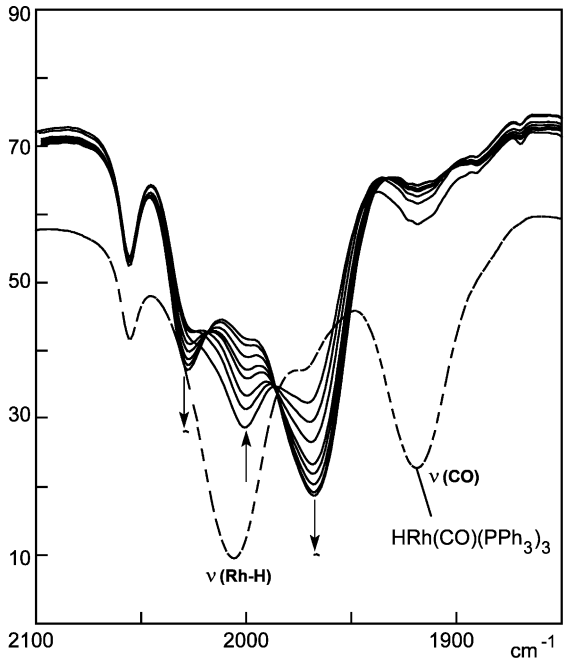

Fig. 2. IR spectra in CH_2Cl_2 measured during the reaction of $HRh(CO)(PPh_3)_3$ with $Ag(CF_3SO_3)$ ([Rh]:[Ag] = 1:0.7). The arrows show decrease (↑) or increase (↓) of the band intensity. $[HRh(CO)(PPh_3)_3]^+$: ν(CO) 2000 cm^{-1}; $[Rh(CO)(PPh_3)_3]^+$: ν(CO) 1970 cm^{-1}; and unidentified product: ν(CO) 2028 cm^{-1}.

small amount of the second unidentified product with ν(CO) 2028 cm^{-1} was also observed. The formation of Rh(I) cationic complex from $[HRh(CO)(PPh_3)_3]^+$ intermediate was accompanied with H_2 evolution. In the test reaction, the gas evolved was introduced to a solution of $[Rh(P(OPh)_3)_4]ClO_4$ in $CDCl_3$, which was next analyzed by ^1H NMR. The presence of a hydrido resonance at $\delta = -9.55$ ppm split into two characteristic multiplets because of a P–H coupling ($J(P–H_{trans}) = 222$ Hz) confirmed the presence of $[RhH_2(P(OPh)_3)_4]ClO_4$ (reaction (4)):

$$[HRh(CO)(PPh_3)_3]^+ \xrightarrow[[Rh(P(OPh)_3)_4]ClO_4]{} [Rh(CO)(PPh_3)_3] \xrightarrow{} [RhH_2(P(OPh)_3)_4]ClO_4 \quad (4)$$

It can be concluded that the IR spectra confirmed the formation of $[Rh(CO)(PPh_3)_3]^+$ complexes during the reaction of $HRh(CO)(PPh_3)_3$ with AgY salts, similarly as it was reported for electrochemical oxidation reaction [4–6]. However, we were not able to isolate these species and in all experiments $[Rh(CO)(PPh_3)_2(H_2O)]^+$ cationic complexes were obtained instead.

2.2. Crystal structure of trans-$Rh(CO)(PPh_3)_2(OPOF_2)$

The unit cell contains two crystallographically independent molecules of the $Rh(CO)(PPh_3)_2(OPOF_2)$ complex. The views of these molecules are depicted in Fig. 1 and selected bond lengths and angles are collected in Table 1. Each molecule consists of a distorted square-planar rhodium center with the PPh_3 groups in *trans* positions and the remaining *trans* positions occupied by carbonyl and the O-bonded difluorophosphate anion. Both molecules display the same eclipsed arrangement of the two phosphine ligands with the carbonyl ligand sandwiched between two phenyl rings. There are marked distortions of the Rh coordination geometry toward

Table 1
Selected geometric parameters (Å, °) for *trans*-$Rh(CO)(PPh_3)_2(OPOF_2)$

Molecule I		Molecule II	
Rh(1)–C(1)	1.794(2)	Rh(2)–C(2)	1.793(2)
Rh(1)–O(11)	2.089(2)	Rh(2)–O(12)	2.091(2)
Rh(1)–P(2)	2.3346(9)	Rh(2)–P(5)	2.3269(9)
Rh(1)–P(1)	2.3359(8)	Rh(2)–P(4)	2.3430(8)
C(1)–O(1)	1.152(3)	C(2)–O(2)	1.155(3)
P(1)–C(13)	1.819(2)	P(4)–C(17)	1.825(2)
P(1)–C(12)	1.824(2)	P(4)–C(18)	1.829(2)
P(1)–C(11)	1.829(2)	P(4)–C(19)	1.835(2)
P(2)–C(16)	1.824(2)	P(5)–C(110)	1.820(2)
P(2)–C(14)	1.825(2)	P(5)–C(111)	1.823(2)
P(2)–C(15)	1.836(3)	P(5)–C(112)	1.827(2)
P(3)–O(11)	1.473(2)	P(6)–O(22)	1.456(2)
P(3)–O(21) [a]	1.481(3)	P(6)–O(12)	1.469(2)
P(3)–F(31) [a]	1.558(2)	P(6)–F(32)	1.546(2)
P(3)–F(41)	1.531(2)	P(6)–F(42)	1.553(2)
C(1)–Rh(1)–O(11)	173.33(9)	C(2)–Rh(2)–O(12)	174.01(9)
C(1)–Rh(1)–P(2)	89.51(8)	C(2)–Rh(2)–P(5)	92.20(8)
O(11)–Rh(1)–P(2)	92.40(5)	O(12)–Rh(2)–P(5)	89.07(5)
C(1)–Rh(1)–P(1)	90.90(8)	C(2)–Rh(2)–P(4)	90.08(7)
O(11)–Rh(1)–P(1)	87.92(5)	O(12)–Rh(2)–P(4)	90.47(5)
P(2)–Rh(1)–P(1)	173.60(2)	P(5)–Rh(2)–P(4)	162.47(2)
O(1)–C(1)–Rh(1)	177.3(2)	O(2)–C(2)–Rh(2)	176.6(2)
C(13)–P(1)–C(12)	104.15(10)	C(17)–P(4)–C(18)	104.07(10)
C(13)–P(1)–C(11)	103.44(10)	C(17)–P(4)–C(19)	106.60(11)
C(12)–P(1)–C(11)	106.88(10)	C(18)–P(4)–C(19)	105.08(10)
C(13)–P(1)–Rh(1)	118.29(7)	C(17)–P(4)–Rh(2)	116.76(8)
C(12)–P(1)–Rh(1)	114.15(7)	C(18)–P(4)–Rh(2)	115.51(7)
C(11)–P(1)–Rh(1)	108.90(7)	C(19)–P(4)–Rh(2)	107.91(8)
C(16)–P(2)–C(14)	106.82(10)	C(110)–P(5)–C(111)	103.52(10)
C(16)–P(2)–C(15)	101.49(11)	C(110)–P(5)–C(112)	105.14(10)
C(14)–P(2)–C(15)	105.87(11)	C(111)–P(5)–C(112)	105.76(11)
C(16)–P(2)–Rh(1)	114.51(8)	C(110)–P(5)–Rh(2)	119.16(8)
C(14)–P(2)–Rh(1)	110.82(7)	C(111)–P(5)–Rh(2)	120.30(8)
C(15)–P(2)–Rh(1)	116.39(8)	C(112)–P(5)–Rh(2)	101.26(7)
P(3)–O(11)–Rh(1)	154.08(12)	P(6)–O(12)–Rh(2)	162.10(11)
O(11)–P(3)–O(21) [a]	120.97(14)	O(12)–P(6)–O(22)	122.70(10)
O(11)–P(3)–F(41)	107.54(11)	O(12)–P(6)–F(32)	106.08(9)
O(11)–P(3)–F(31) [a]	106.24(11)	O(12)–P(6)–F(42)	106.61(9)
O(21) [a]–P(3)–F(41)	116.7(2)	O(22)–P(6)–F(42)	110.23(10)
O(21) [a]–P(3)–F(31) [a]	105.69(15)	O(22)–P(6)–F(32)	110.54(10)
F(41)–P(3)–F(31) [a]	96.21(12)	F(32)–P(6)–F(42)	97.74(10)

[a] Occupancy: 0.77.

tetrahedral in the two independent molecules, evident both from the P–Rh–P and C–Rh–O angles of 173.60(2)° and 173.33(9)° for Rh(1), and of 162.47(2)° and 174.01(9)° for Rh(2) as well as from the displacement of the donor atoms from their mean plane by up to approximately 0.12 Å for atoms bonded to Rh(1) and up to approximately 0.24 Å for atoms bonded to Rh(2). Additionally, the Rh(2) atom is displaced by approximately 0.12 Å out of the mean plane of its donor atoms. All Rh–P, Rh–C, and C–O bond distances are within the ranges found for other complexes of the *trans*-$Rh(PPh_3)_2(CO)$L-type [14–19], where L is a neutral molecule (H_2O, CH_3CN) or anion (Cl^-, ClO_3^-, HCO_2^-, $CF_3CO_2^-$, PhO^-). The mean Rh–O distance of 2.090(2) Å, found in the present structure, lies between 2.130–2.115 Å found for H_2O and 2.022–2.075 Å found for the O-bonded anions mentioned above. The geometry of the two independent $OPOF_2^-$ anions is that previously found [13] and it exhibits an enlargement of the O–P–O angle and a contraction of the F–P–F angle in relation to the ideal tetrahedral value of 109.5° in accordance with the VSEPR rules [20]. Due to a disorder, the geometry of the $OPOF_2^-$ group attached to Rh(1) is somewhat distorted. All the four independent PPh_3 groups show significant deviations from cylindrical symmetry about the Rh–PPh_3 bond axis, as can be seen from Fig. 1. Although the mean values of the P–C bond distances and the Rh–P–C and C–P–C angles for each of the four groups (1.825(5) Å, 114° and 105°, respectively) are as expected, there exist considerable variations in the angular parameters, the Rh(2)–P(5)–C angles being the largest at 101.2(1)–120.3(1)°.

The only remarkable differences between the chemically equivalent bond lengths in the two complex molecules are those in the Rh–P bond lengths (a statistically significant difference is observed for two Rh(2)–P bond lengths of 2.3269(9) and 2.3430(7) Å), whereas significant conformational and angular differences make the two molecules considerably different, in spite of general similarities. The most striking difference between the two molecules concerns the arrangement of the $OPOF_2^-$ anion with respect to the coordination core of each molecule, evident from the values of the Rh–O–P angles (154.1(2)° for Rh(1) and 162.1(1)° for Rh(2)) and from the values of the Rh–O–P–O torsion angles (ca. −160° and +120°, respectively, for the main and minor components of Rh(1) and 83° for Rh(2)). This is connected with a different pattern of intra- and intermolecular C–H...O hydrogen bonds in which the two oxygen atoms of each $OPOF_2^-$ anion participate (see Table 2). The intramolecular hydrogen bonds are depicted in Fig. 1. It seems that, while the rotation of the anion about the Rh–O bond is restricted by the intramolecular hydrogen bonds involving the O atom (O(11) or O(12)) bonded to the Rh atom, its orientation about the O–P bond depends rather on the intermolecular ones, which involve the terminal O atom (O(21), O(211), and O(22)). It should be noted that the arrangement of the anion bonded to Rh(2) causes more repulsion in the molecule as indicated by deformations of bond lengths and angles being larger at Rh(2) than at Rh(1). Therefore, the conformation of the complex molecule containing Rh(2), as probably forced by intermolecular interactions, should not be retained in a solution.

Table 2
Hydrogen bond like close contacts (Å, °) for *trans*-$Rh(CO)(PPh_3)_2(OPOF_2)$

D–H...A	d(H...A)	d(D...A)	<(DHA)
C(23)–H(23)...O(11)	2.50	3.286(3)	141
C(66)–H(66)...O(11)	2.63	3.357(3)	133
C(212)–H(212)...O(22)	2.65	3.427(3)	139
C(67)–H(67)...O(12)	2.56	3.277(3)	133
C(69)–H(69)...Rh(2)	2.72	3.360(3)	126
C(35)–H(35)...Rh(2)	3.03	3.923(3)	157
C(511)–H(511)...Rh(1)	3.17	3.973(3)	144
C(33)–H(33)...O(1) [a]	2.52	3.138(3)	123
C(43)–H(43)...O(1) [a]	2.58	3.169(3)	121
C(47)–H(47)...O(2) [b]	2.58	3.176(3)	121
C(57)–H(57)...O(2) [b]	2.65	3.211(3)	118
C(39)–H(39)...O(21) [c,d]	2.50	3.317(4)	144
C(42)–H(42)...O(22) [e]	2.42	3.318(3)	158
C(48)–H(48)...O(211) [f,g]	2.56	3.281(8)	133
C(46)–H(46)...O(211) [f,g]	2.65	3.305(8)	127

[a] Symmetry transformations used to generate equivalent atoms: $x-1, y, z$.
[b] Symmetry transformations used to generate equivalent atoms: $x+1, y, z$.
[c] Occupancy: 0.23.
[d] Symmetry transformations used to generate equivalent atoms: $x+1, y+1, z$.
[e] Symmetry transformations used to generate equivalent atoms: $-x+1, y-1/2, -z$.
[f] Occupancy: 0.77.
[g] Symmetry transformations used to generate equivalent atoms: $-x, y+1/2, -z+1$.

An interesting feature of the crystal structure is the presence of an approximate center of symmetry at about 0.23, 0.73, and 0.26, which relates more exactly the coordinates of the interior portions of the two complex molecules than the external portions. These molecules are arranged in such a way that the C–H bond of one phenyl ring from each molecule points towards the Rh atom of the other molecule. The Rh...H lines are nearly perpendicular to the ligand coordination mean plane, but the relevant distances of 3.03–3.17 Å are rather long for C–H...Rh hydrogen bonds. However, an approach of pseudo-symmetry-related molecules causes steric interactions between their phenyl groups and is responsible for the bending of the phosphine groups away from the adjacent molecule and for distortions of the Rh–P–C angles. Adjacent pairs of non-equivalent molecules

are joined by C–H...O interactions involving $OPOF_2^-$ anions and carbonyl ligands.

2.3. Reactions of $HRh(CO)(P(OPh)_3)_3$ and $HRh(P(OPh)_3)_4$ complexes with AgY salts ($Y = PF_6^-$, $CF_3SO_3^-$, BF_4^-)

The IR spectrum of the $HRh(CO)(P(OPh)_3)_3$ starting complex in CH_2Cl_2 solution contains an intense ν(CO) band at 2056 cm^{-1} and a broad band at approximately 1970 cm^{-1} assigned to ν(Rh–H). After Ag(I) salt addition, first a new ν(CO) band appeared at 2075 cm^{-1}, and then shifted to 2083 cm^{-1}. At the same time, changes in the region of ν(Rh–H) frequencies were observed; the initial band at 1970 cm^{-1} was shifted to 1965 cm^{-1} and became narrow and more intense. These changes, as well as precipitation of silver metal, suggest the formation of the $[HRh(CO)(P(OPh)_3)_3]^+$ complex, which was confirmed by the ESR spectrum measured in frozen CH_2Cl_2 solution. This ESR spectrum, similar to that reported for $[HRh(CO)(PPh_3)_3]^+$ [4], is consistent with the square-pyramidal structure of complex with an apical phosphorus ligand. The values of hyperfine coupling constants for phosphorus are $A_1 = 332$ G, $A_2 = 324$ G, and $A_3 = 364$ G, and are remarkably higher than those observed for $[HRh(CO)(PPh_3)_3]^+$, reflecting the weaker basicity of $P(OPh)_3$ compared with that of PPh_3 [21].

The $[HRh(CO)(P(OPh)_3)_3]Y$ intermediate species decomposed with H_2 evolution to $[Rh(CO)(P(OPh)_3)_3]Y$ ($Y = PF_6^-$, BF_4^-, $CF_3SO_3^-$) complexes, which have been isolated and characterized (reaction (5)):

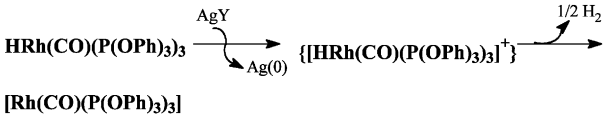

(5)

Following this reaction pattern, one may observe significant difference in reactivity of $[Rh(CO)L_3]^+$ cationic complexes with PPh_3 and $P(OPh)_3$ ligands (compare reaction (1) with reaction (5)).

Complexes of $[Rh(CO)(P(OPh)_3)_3]Y$ formula presented ^{31}P NMR spectra with the typical A_2BX pattern (A, B = ^{31}P; X = ^{103}Rh) with parameters practically independent on the kind of anion Y. The difference between the two J(Rh–P) coupling constant values is equal (ca. 20 Hz) and is smaller than that in the ^{31}P NMR spectra of $RhX(P(OPh)_3)_3$ complexes (Table 3) [22]. An intense ν(CO) band was observed at 2083 cm^{-1} (in KBr and in CH_2Cl_2). When CH_2Cl_2 solution of $[Rh(CO)(P(OPh)_3)_3]PF_6$ was saturated with CO, the second CO ligand was coordinated to rhodium and second intense ν(CO) band appeared at 2032 cm^{-1}. This spectrum was identical with that obtained for a solution of $[Rh(P(OPh)_3)_4]ClO_4$ in CH_2Cl_2 saturated with CO and consistent with the presence of the $[Rh(CO)_2(P(OPh)_3)_3]^+$ cation [22].

Table 3
Selected ^{31}P NMR (J(Rh–P), Hz) data of complexes $[Rh(CO)(P(OPh)_3)_3]Y$, $[Rh(P(OPh)_3)_4]Y$, and $RhX(P(OPh)_3)_3$ in $CDCl_3$

Y or X	$[Rh(CO)(P(OPh)_3)_3]Y$	$[Rh(P(OPh)_3)_4]Y$	$RhX(P(OPh)_3)_3$
PF_6	199.3; 222.0	213.6	
CF_3SO_3	200.0; 217.0		
BF_4	200.8; 220.6		
Cl [22]			224.0; 285.0
NCS [22]			220.6; 266.2
CN [22]			225.3; 224.2

The exchange of $P(OPh)_3$ and CO ligands in the coordination sphere of rhodium can easily be monitored by IR or UV–Vis spectroscopy. For example, the transformation of $[Rh(CO)(P(OPh)_3)_3]PF_6$ to $[Rh(P(OPh)_3)_4]PF_6$ in the presence of free $P(OPh)_3$ (reaction (6)) is quantitative and accompanied by the disappearance of ν(CO) in the IR spectrum as well as by the shift of the absorption band in UV–Vis from 396 to 382 nm:

$$[Rh(CO)(P(OPh)_3)_3]^+ \xrightarrow{P(OPh)_3} [Rh(P(OPh)_3)_4]^+ + CO \quad (6)$$

The reaction of the hydrido complex $HRh(P(OPh)_3)_4$ with $AgPF_6$ was performed for comparison with above-studied reactions. The ESR measurement of the frozen reaction solution containing 1 equiv. of silver per rhodium confirmed the formation of an Rh(II) complex, $[HRh(P(OPh)_3)_4]^+$, with square-pyramidal symmetry. The spectrum presented two sets of lines with parameters very similar to those for $[HRh(CO)(P(OPh)_3)_3]^+$. The final reaction product, $[Rh(P(OPh)_3)_4]PF_6$, was identified by means of ^{31}P NMR ($\delta = 105.4$ ppm,

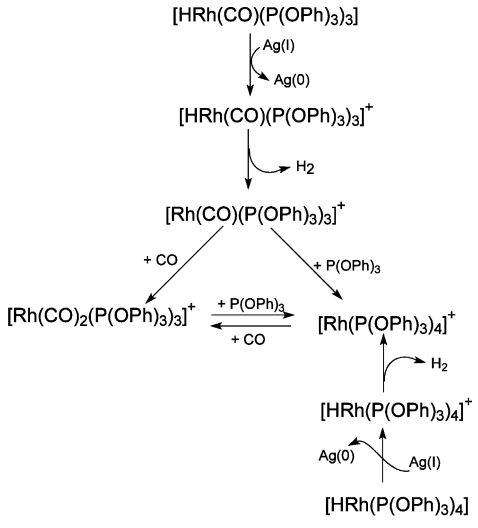

Scheme 2.

J(Rh–P) = 213.6 Hz) and UV–Vis spectra, close to those of the analogous complexes, $[Rh(P(OPh)_3)_4]ClO_4$ and $[Rh(P(OPh)_3)_4]BPh_4$, respectively (see Scheme 2) [23].

3. Conclusions

The $HRh(CO)L_3$ complexes ($L = PPh_3$, $P(OPh)_3$) are oxidized with AgY salts to $[HRh(CO)L_3]^+$ species, identified in solution by ESR and IR spectra. These Rh(II) intermediates decompose with H_2 evolution forming Rh(I) cationic complexes, $[Rh(CO)L_3]^+$. The $[Rh(CO)(PPh_3)_3]^+$ complexes exist only in solution and during isolation procedure at presence of even traces of water are converted to $[Rh(CO)(PPh_3)_2(H_2O)]^+$ complexes. In contrast, analogous phosphito complexes of $[Rh(CO)(P(OPh)_3)_3]^+$ structure are stable and can be isolated in solid.

4. Experimental

4.1. Reactants

The following rhodium complexes $HRh(CO)(PPh_3)_3$ [24], $HRh(CO)(P(OPh)_3)_3$ [25], and $[Rh(P(OPh)_3)_4]ClO_4$ were prepared by literature methods [23]. $AgPF_6$ and $Ag(CF_3SO_3)$ were purchased from Aldrich and $AgBF_4$ from Avocado Research Chemicals. CH_2Cl_2 was distilled from CaH_2 and stored under dinitrogen. All reactions of rhodium complexes with silver salts were performed under N_2 using the standard Schlenk technique.

4.2. Rhodium complex syntheses and identification

4.2.1. $[Rh(CO)(PPh_3)_2(H_2O)]BF_4$

To the solution of 0.03 g (1.5×10^{-4} mol) of $AgBF_4$ in 3 ml of CH_2Cl_2, 0.10 g (1.1×10^{-4} mol) of $HRh(CO)(PPh_3)_3$ was added and the mixture was stirred for 15 min. The dark reddish-brown solution was filtered to remove precipitate of silver metal and evaporated to dryness under vacuum. The yellowish-brown solid was washed with ethyl ether and dried.

^{31}P NMR ($CDCl_3$; δ, ppm) 26.3, J(Rh–P) = 128.2 Hz; IR (KBr; cm^{-1}): 1993 vs (ν(CO)), 1100 (BF_4), CH_2Cl_2: 1998; UV–Vis ($CHCl_3$, nm) 274, 348; MS (m/z): 655 ($Rh(PPh_3)_2(CO)^+$), 627 ($Rh(PPh_3)_2^+$).

4.2.2. $[Rh(CO)(PPh_3)_2(H_2O)]CF_3SO_3$

Complex was obtained following above procedure using 0.04 g (1.6×10^{-4} mol) of $AgCF_3SO_3$ and 0.1 g (1.1×10^{-4} mol) of $HRh(CO)(PPh_3)_3$. ^{31}P NMR ($CDCl_3$; δ, ppm) 29.8, d, J(Rh–P) = 124.0 Hz; IR (KBr; cm^{-1}): 1993 vs, 2011 s (ν(CO)), CH_2Cl_2: 1998.

4.2.3. $[Rh(CO)(PPh_3)_2(H_2O)]PF_6$

Complex was obtained as above using 0.064 g (2.5×10^{-4} mol) of $AgPF_6$ and 0.22 g (2.4×10^{-4} mol) of $HRh(CO)(PPh_3)_3$. ^{31}P NMR ($CDCl_3$; δ, ppm) 26.0, d, J(Rh–P) = 125.1 Hz; −146.9, J(P–F) = 714 Hz (PF_6); IR (KBr; cm^{-1}): 1997 vs (ν(CO)), 850 (PF_6); UV–Vis ($CHCl_3$; nm) 278, 346; MS (m/z): 655 ($Rh(PPh_3)_2(CO)^+$), 627 ($Rh(PPh_3)_2^+$).

4.2.4. $Rh(CO)(PPh_3)_2(OPOF_2)$

A sample of $[Rh(CO)(PPh_3)_2(H_2O)]PF_6$, approximately 0.03 g ($3.7 \times 10^{-4}$ mol), was dissolved in ethanol (2 ml) and left for crystallization. After 3 days, orange crystals were obtained. Found: C, 58.06; H, 4.4. $C_{37}H_{30}F_2P_3O_3Rh$ requires C, 58.75; H, 4.4%. ^{31}P NMR ($CDCl_3$; δ, ppm) 25.9, d, J(Rh–P) = 125 Hz; −20.9, t, J(P–F) = 960 Hz; IR (KBr; cm^{-1}): 1984 vs (ν(CO)), 1300 s (ν(PO)).

4.2.5. $[Rh(CO)(P(OPh)_3)_3]BF_4$

To the solution of 0.03 g (1.5×10^{-4} mol) of $AgBF_4$ in 2 ml of CH_2Cl_2, 0.11 g (1.0×10^{-4} mol) of $HRh(CO)(P(OPh)_3)_3$ was added and the mixture was stirred for 30 min. The yellow solution was filtered to remove silver metal and evaporated to dryness under vacuum. The resulted pale yellow powder was washed with methanol and dried. Found: C, 57.35; H, 3.93. $C_{55}H_{45}BF_4P_3O_{10}Rh$ requires C, 57.52; H, 3.95%. ^{31}P NMR ($CDCl_3$; δ, ppm) A_2BX: 109.6 (P_A), J(Rh–P) = 200.8 Hz, 106.7 (P_B), J(Rh–P) = 220.6 Hz, J(P–P) = 62.1 Hz; IR (KBr; cm^{-1}): 2083 ν(CO), 1080 (BF_4); UV–Vis ($CHCl_3$; nm) 296, 396; MS (m/z): 1033 ($Rh(P(OPh)_3)_3^+$), 724 ($Rh(P(OPh)_3)_2^+$).

4.2.6. $[Rh(CO)(P(OPh)_3)_3]CF_3SO_3$

Complex was obtained as above using 0.05 g (2.0×10^{-4} mol) of $Ag(CF_3SO_3)$ and 0.18 g (1.7×10^{-4} mol) of $HRh(CO)(P(OPh)_3)_3$ in 4 ml of CH_2Cl_2. The yellow powder obtained was washed with methanol and dried. Found: C, 55.36; H, 3.43. $C_{56}H_{45}F_3SP_3O_{13}Rh$ requires C, 55.55; H, 3.75%. ^{31}P NMR ($CDCl_3$; δ, ppm) A_2BX: 113.0 (P_A), J(Rh–P) = 200.0 Hz, 110.0 (P_B), J(Rh–P) = 217.0 Hz, J(P–P) = 63 Hz; IR (KBr; cm^{-1}): 2083 ν(CO), 1080 (BF_4); UV–Vis ($CHCl_3$; nm) 296, 396; MS (m/z): 1033 ($Rh(P(OPh)_3)_3^+$), 724 ($Rh(P(OPh)_3)_2^+$).

4.2.7. $[Rh(CO)(P(OPh)_3)_3]PF_6$

Complex was obtained as above using 0.05 g (2.0×10^{-4} mol) of $AgPF_6$ and 0.18 g (1.7×10^{-4} mol) of $HRh(CO)(P(OPh)_3)_3$. The pale yellow powder obtained was washed with methanol and dried. Found: C, 54.45; H, 3.13. $C_{55}H_{45}F_6P_4O_{10}Rh$ requires C, 54.74; H, 3.76%. ^{31}P NMR ($CDCl_3$; δ, ppm) A_2BX: 109.6 (P_A), J(Rh–P) = 199.3 Hz, 106.7 (P_B), J(Rh–P) = 222 Hz, J(P–

P) = 61.8 Hz; −147, J(P–F) = 714 Hz (PF_6); IR (KBr; cm^{-1}): 2085 ν(CO), 840 (PF_6); UV–Vis ($CHCl_3$; nm) 296, 396; MS (m/z): 1033 ($Rh(P(OPh)_3)_3^+$), 724 ($Rh(P(OPh)_3)_2^+$).

4.2.8. [Rh(P(OPh)3)4]PF6

Complex was obtained as above using 0.012 g (4.8×10^{-5} mol) of $AgPF_6$ and 0.05 g (3.7×10^{-5} mol) of $HRh(P(OPh)_3)_4$. The pale yellow product was obtained by evaporation to dryness of the reaction solution after separation of silver metal. Found: C, 54.25; H, 3.13. $C_{55}H_{45}F_6P_4O_{10}Rh$ requires C, 54.74; H, 3.76%. ^{31}P NMR ($CDCl_3$; δ, ppm): 105.4, d, J(Rh–P) = 213.6 Hz, −146.9, J(P–F) = 711 Hz (PF_6); UV–Vis ($CHCl_3$; nm) 294, 382.

4.2.9. ESR data of Rh(II) complexes in CH_2Cl_2 solution

$[HRh(CO)(P(OPh)_3)_3]^+$ (77 K): $g_1 = 2.23$, $g_2 = 2.195$, $g_3 = 2.118$; $A(P_{ap})_1 = 332$ G, $A(P_{ap})_2 = 324$ G, $A(P_{ap})_3 = 364$ G (the hyperfine couplings were not determined because of poor resolution of the spectrum).

$[HRh(P(OPh)_3)_4]^+$ (77 K): $g_1 = 2.23$, $g_2 = 2.20$, $g_3 = 2.13$; $A(P_{ap})_1 = 337$ G, $A(P_{ap})_2 = 326$ G, $A(P_{ap})_3 = 373$ G (the hyperfine couplings were not determined because of poor resolution of the spectrum).

4.3. Crystal structure determination

Diffraction data were collected on a Kuma KM4CCD area detector diffractometer (ω-scan) with graphite-monochromated Mo Kα radiation ($\lambda = 0.71073$ Å, from a crystal of dimensions approximately 0.25 mm × 0.25 mm × 0.10 mm). 53 110 reflections (17 191 unique) were measured to $2\Theta = 60^\circ$ (h: −13 → 13, k: −21 → 19, l: −29 → 31). The numerical, face indexed, correction for absorption was applied ($T_{min} = 0.824$, $T_{max} = 0.925$ [26]). The structure was solved using direct methods with SHELXS97 [27] and refined by the full-matrix least-squares method on all the F^2 data using SHELXL97 [28]. Systematic absences correspond $P2_1$ and $P2_1/m$ space groups. Non-centrosymmetric $P2_1$ space group was concluded from statistics for the normalized structure factors ($|E^2-1| = 0.750$) and confirmed by the successful structure analysis. The refinement of the Flack parameter [29] based on 7273 Friedel opposites indicated racemic twining with 0.28 fraction of the inverted structure. One of the two independent $OPOF_2^-$ groups was found to be rotationally disordered between two conformations refined with 0.77 occupancy for O(21) and F(31) and 0.23 occupancy for O(211) and F(311). One fluorine F(41) is common to both conformations in our model. All non-hydrogen atoms, except of F(311) and O(211), were refined with anisotropic displacement parameters. These parameters are large and directional for the O(21) and F(41) atoms of the disordered group and for the atoms of the phenyl ring C(16)–C(56), neighboring to this group. The hydrogen atoms were included in calculated positions (C–H: 0.95 Å) with isotropic displacement parameters set at $1.2U_{eq}$ of the bonded carbon atom. Scattering factors were taken from Ref. [30].

Crystal data: $C_{37}H_{30}F_2O_3P_3Rh$, $M = 756.43$, monoclinic, space group $P2_1$, $a = 9.914(3)$ Å, $b = 15.198(3)$ Å, $c = 22.228(4)$ Å, $\beta = 98.89(3)^\circ$, $V = 3308.9(13)$ Å^3, $Z = 4$, $T = 100(2)$ K, $\mu = 0.709$ mm^{-1}, $F(000) = 1536$, 53 110 reflections measured, 17 190 unique ($R_{int} = 0.034$), $wR_2(F^2) = 0.0493$ (all data), $R_1 = 0.0290$ [$I > 2\sigma(I)$], $S = 1.006$.

4.4. Measurements

UV–Vis spectra have been measured on Hewlett-Packard 8452 Diode Array spectrometer, IR spectra were recorded on Nicolet Impact 400, and NMR spectra on Bruker 300 spectrometers. ESR spectra have been measured on Electron Spin Resonance ESP 300 E Bruker spectrometer.

Acknowledgements

We are indebted to Prof. Armando Pombeiro for helpful discussion. Grant No. PBZ-KBN 15/09/T09/99/01d is gratefully acknowledged.

References

[1] B. Cornils, W.A. Herrmann (Eds.), Applied Homogeneous Catalysis with Organometallic Compounds: A Comprehensive Handbook in Two Volumes, VCH, Weinheim, 1996.
[2] A.M. Trzeciak, J.J. Ziólkowski, Coord. Chem. Rev. 190–192 (1999) 883.
[3] H.K.A.C.R. Coolen, J.M. Nolte, P.W.N.M. van Leeuwen, J. Organomet. Chem. 496 (1995) 159.
[4] D. Menglet, A.M. Bond, K. Coutinho, R.S. Dickson, G.G. Lazarev, S.A. Olsen, J.P. Pilbrow, J. Am. Chem. Soc. 120 (1998) 2086.
[5] G. Pilloni, G. Schiavon, G. Zotti, S. Zecchin, J. Organomet. Chem. 134 (1977) 305.
[6] S. Valcher, G. Pilloni, M. Martelli, J. Electroanal. Chem. 42 (1973) App. 5.
[7] R.R. Schrock, J.A. Osborn, J. Am. Chem. Soc. 93 (1971) 2397.
[8] P. Legzdins, R.W. Mitchel, G.L. Rempel, J.D. Fuddick, G. Wilkinson, J. Am. Chem. Soc. A (1970) 3322.
[9] D.M. Branan, N.W. Hoffman, E.A. McElroy, N. Prokopuk, A.B. Salazar, M.J. Robbins, W.E. Hill, T.R. Webb, Inorg. Chem. 30 (1991) 1200.
[10] A. Svetlanova-Larsen, J.L. Hubbard, Inorg. Chem. 35 (1996) 3073.
[11] N.G. Connelly, T. Einig, G. Garcia Herbosa, P.M. Hopkins, C. Mealli, A.G. Orpen, G.M. Rosair, F. Viguri, J. Chem. Soc., Dalton Trans. (1994) 2025.

[12] C. White, S.J. Thompson, P.M. Maitlis, J. Organomet. Chem. 134 (1977) 319.
[13] D.L. Reger, M.F. Huff, L. Lebioda, Acta Crystallogr., C 47 (1991) 1167.
[14] A.L. Rheingold, S.J. Geib, Acta Crystallogr., Sect. C 43 (1987) 784.
[15] K.R. Dunbar, S.C. Haefner, Inorg. Chem. 31 (1992) 3676.
[16] C.J. Davies, I.M. Dodd, M.M. Harding, B.T. Heaton, C. Jacob, J. Ratnam, J. Chem. Soc., Dalton Trans. (1994) 787.
[17] S.F. Hossain, K.M. Nicholas, C.L. Teas, R.E. Davis, Chem. Commun. (1981) 268.
[18] W.I. Sokol, N.F. Golgshleger, M.A. Poraj-Koshic, Koord. Hhim. 19 (1993) 47.
[19] K.A. Bernard, M.R. Churchill, T.S. Janik, J.D. Atwood, Organometallics 9 (1990) 12.
[20] R.J. Gillespie, J. Chem. Educ. 40 (1963) 295.
[21] C.A. Tolman, Chem. Rev. 77 (1977) 313.
[22] A.M. Trzeciak, J.J. Ziólkowski, Transition Met. Chem. 14 (1989) 135.
[23] L.M. Haines, Inorg. Chem. 9 (1970) 1517.
[24] D. Evans, G. Yagupsky, G. Wilkinson, J. Chem. Soc. A (1968) 2660.
[25] A.M. Trzeciak, J. Organomet. Chem. 390 (1990) 105.
[26] Kuma Kuma Diffraction (1995–1999), KM4CCd Software, Version 1.166, Kuma Diffraction Instruments GmbH, Wroclaw, Poland.
[27] G.M. Sheldrick, SHELXS97, Program for the Solution of Crystal Structures, Universität Göttingen, Göttingen, Germany, 1997.
[28] G.M. Sheldrick, SHELXL97, Program for the Refinement of Crystal Structures, Universität Göttingen, Göttingen, Germany, 1997.
[29] H.D. Flack, Acta Crystallogr., A 39 (1983) 876.
[30] A.J.C. Wilson, International Tables for Crystallography, vol. C, Kluwer Academic Publishers, Dordrecht, 1992.